

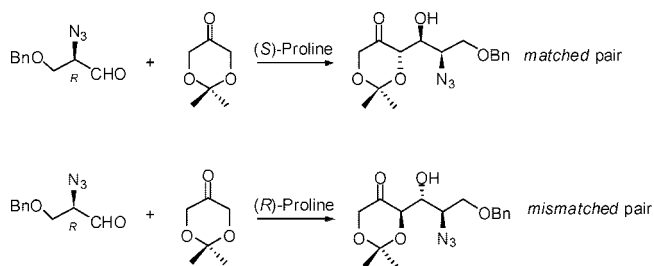
## Origins of the Double Asymmetric Induction on Proline-Catalyzed Aldol Reactions

Félix Calderón,<sup>†</sup> Elisa G. Doyagüez,<sup>†</sup> Paul Ha-Yeon Cheong,<sup>‡</sup>  
Alfonso Fernández-Mayoralas,<sup>\*,†</sup> and K. N. Houk<sup>\*,‡</sup>

*Instituto de Química Orgánica General, CSIC, Juan de la Cierva 3, 28006 Madrid, Spain, and  
Department of Chemistry and Biochemistry, University of California, Los Angeles, California 90095-1569*

*mayoralas@iqog.csic.es; houk@chem.ucla.edu*

*Received May 14, 2008*



Computational studies to elucidate the origin of the double asymmetric induction on proline-catalyzed aldol reaction have been performed using HF/6-31G(d) calculations. The computed transition structures explain the experimental data obtained.

### Introduction

From the discoveries of Hajos, Parrish, Eder, Sauer, and Wiechert<sup>1,2</sup> in the early 1970s, to the recent discoveries of List, Barbas, and Lerner,<sup>3,4</sup> the proline-catalyzed aldol reaction has been shown to be a versatile method for C–C bond formation. Interesting asymmetric syntheses have been accomplished using this methodology, such as the synthesis of carbohydrates, steroids, and useful building blocks.<sup>5</sup> We have recently contributed to this field by reporting a novel synthesis of six-membered azasugars from diethyl tartrate (**1**), where the key step is a proline-catalyzed aldol reaction between the chiral aldehyde **2** with dioxanone **3** (Scheme 1).<sup>6</sup> During the course of this study we observed an interesting double asymmetric

induction. When (*R*)-aldehyde **2** and ketone **3** reacted in the presence of (*S*)-proline, *anti*-(*S*, *S*) aldol **4** was the only product obtained. However, (*R*)-proline catalysis afforded the *anti*-(*R*, *R*) aldol as major product with lower stereoselectivity (d.r. 5:1). This topicity was confirmed when the aldehyde enantiomer *ent*-**2** was used, affording the enantiomeric aldol products. These results indicate that the inherent selectivities of the two chiral species are mutually reinforcing with the (*R*)-aldehyde/(*S*)-proline or with (*S*)-aldehyde/(*R*)-proline matched pairs. The mismatched case results upon reversing the absolute configuration of either of the two chiral components.

We observed similar effects in the synthesis of 5-membered ring azasugars **15**, a potent  $\alpha$ -galactosidase inhibitor (Scheme 2).<sup>7,8</sup> The reaction of **8** and **3** was first tried following the described conditions,<sup>6</sup> however very low yields of desired products were obtained. It is known that enamine-based direct cross-aldol reactions involving linear aldehydes as acceptor and ketones as donor is difficult.<sup>9</sup> The problem lies in the difficulties for the catalyst to differentiate between the aldehyde and the ketone to form the nucleophilic enamine, resulting in undesirable aldehyde-aldehyde dimers. To overcome this problem, the aldehyde was slowly added to a preformed solution of proline

<sup>†</sup> CSIC.

<sup>‡</sup> University of California.

(1) (a) Hajos, Z. G.; Parrish, D. R. *J. Org. Chem.* **1973**, *38*, 3239–3243. (b) Hajos, Z. G.; Parrish, D. R. *J. Org. Chem.* **1974**, *39*, 1615–1621.

(2) (a) Eder, U.; Sauer, G.; Wiechert, R. *Angew. Chem., Int. Ed. Engl.* **1971**, *10*, 496–497.

(3) (a) List, B.; Lerner, R. A.; Barbas, C. F., III. *J. Am. Chem. Soc.* **2000**, *122*, 2395–2396. (b) Notz, W.; List, B. *J. Am. Chem. Soc.* **2000**, *122*, 7386–7387. (c) Bui, T.; Carbas, C. F., III. *Tetrahedron Lett.* **2000**, *41*, 6951–6954. (d) Sakthivel, K.; Notz, W.; Bui, T.; Barbas, C. F., III. *J. Am. Chem. Soc.* **2001**, *123*, 5260–5267.

(4) For a complete revision see: (a) Alleman, C.; Gordillo, R.; Clemente, F. R.; Ha-Yeon Cheong, P.; Houk, K. N. *Acc. Chem. Res.* **2004**, *37*, 558–569.

(5) (a) Berkessel, A.; Gröger, H. In *Asymmetric Organocatalysis*; VCH: Weinheim, 2004. (b) Dalko, P. I.; Moisan, L. *Angew. Chem., Int. Ed.* **2004**, *43*, 5138–5175. (c) Calderón, F.; Fernández, R.; Sánchez, F.; Fernández-Mayoralas, A. *Adv. Synth. Cat.* **2005**, *347*, 1395–1403.

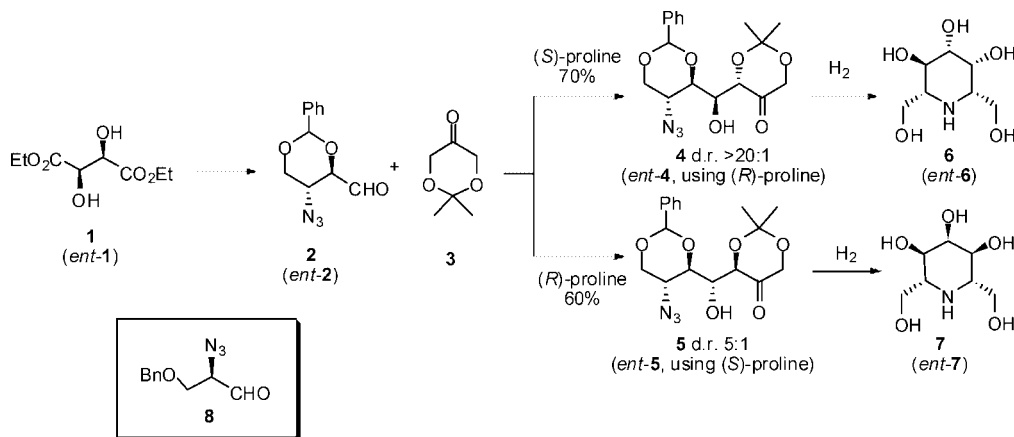
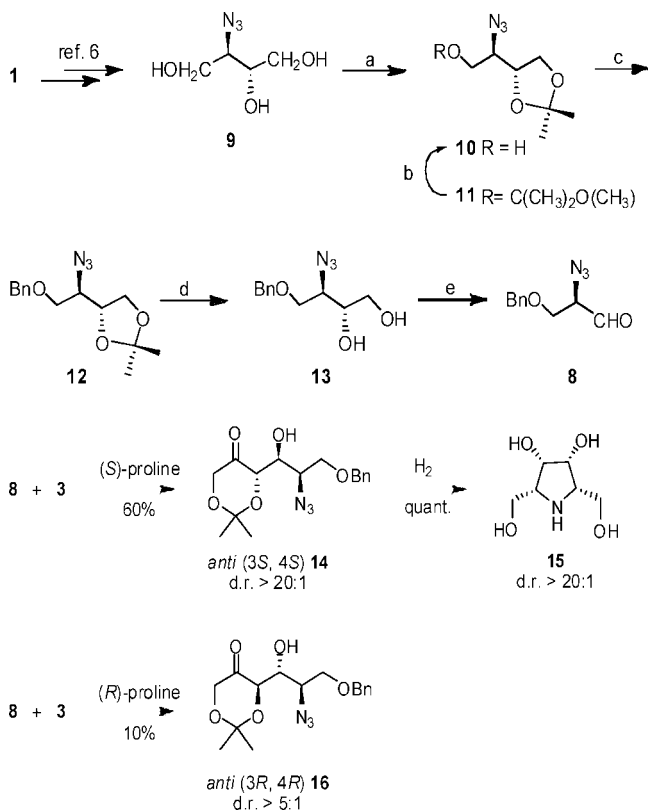
(6) Calderón, F.; Doyagüez, E. G.; Fernández-Mayoralas, A. *J. Org. Chem.* **2006**, *71*, 6258–6261.

(7) Stütz, A. E. In *Iminosugars as Glycosidase Inhibitors: Nojirimycin and Beyond*; Wiley-VCH: Weinheim, Germany, 1999.

(8) Mengel, A.; Reiser, O. *Chem. Rev.* **1999**, *99*, 1191–1223.

(9) List, B.; Pojarliev, P.; Castello, C. *Org. Lett.* **2001**, *3*, 573–575.

## SCHEME 1. Synthesis of Azasugars from Diethyltartrate

SCHEME 2<sup>a</sup>

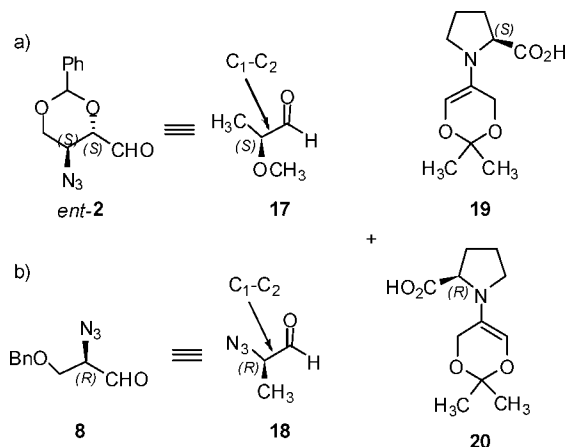
<sup>a</sup> Reaction conditions: (a) *p*-TsOH, 2,2-dimethoxypropane, 24 h, r.t., 50%; (b) PPTS, DMF, 2 h, r.t., 100%; (c) BnBr, NaH, 3 h, r.t., 85%. (d) HCl, MeOH, 2 h, r.t., 82%; (e) NaIO<sub>4</sub>, MeOH/water, 75 min, r.t., 83%.

and ketone. Using this protocol, the reaction of **8** and **3** in the presence of (*S*)-proline gave *anti*-(3*S*, 4*S*)-aldol **14** with good yield (60%), Scheme 2) and excellent stereoselectivity (d.r. > 20:1). On the other hand, the reaction of **8** and **3** in the presence of (*R*)-proline gave *anti*-(3*R*, 4*R*)-aldol **16** as major product but with low yield (10%) and moderate stereoselectivity (d.r. 5:1).

## Results and Discussions

To explain the origins of the double asymmetric induction of these proline-catalyzed aldol additions, we explored the stereoselectivity of this reaction using quantum mechanical calculations on a model system. The  $\alpha$ -hydroxy aldehyde *ent*-**2** was modeled with (*S*)-2-methoxypropanal **17** (Scheme 3a), and

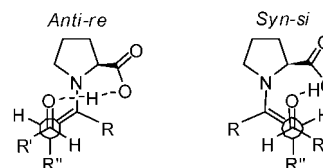
## SCHEME 3. Model System for Theoretical Study



$\alpha$ -azide aldehyde **8** was modeled with (*R*)-2-azidopropanal **18** (Scheme 3b). The three rotamers of **17** and **18**, involving the rotation around C<sub>1</sub>–C<sub>2</sub> bond, were studied. The reaction of these model electrophiles and the (*S*)- and (*R*)-proline-enamine of dioxanone **19** and **20** were computed using HF/6-31G\* calculations.<sup>10</sup> The influence of the enamine ring conformation in the course of the nucleophilic attack was studied for all cases using semiempirical PM3.

Previous quantum mechanical studies have shown that the proline aldol mechanism involves a nucleophilic attack of

## a) Forming C-C bond Newman Projection



## b) Partial-Zimmerman-Traxler TS

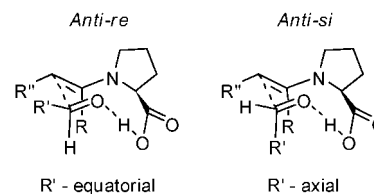
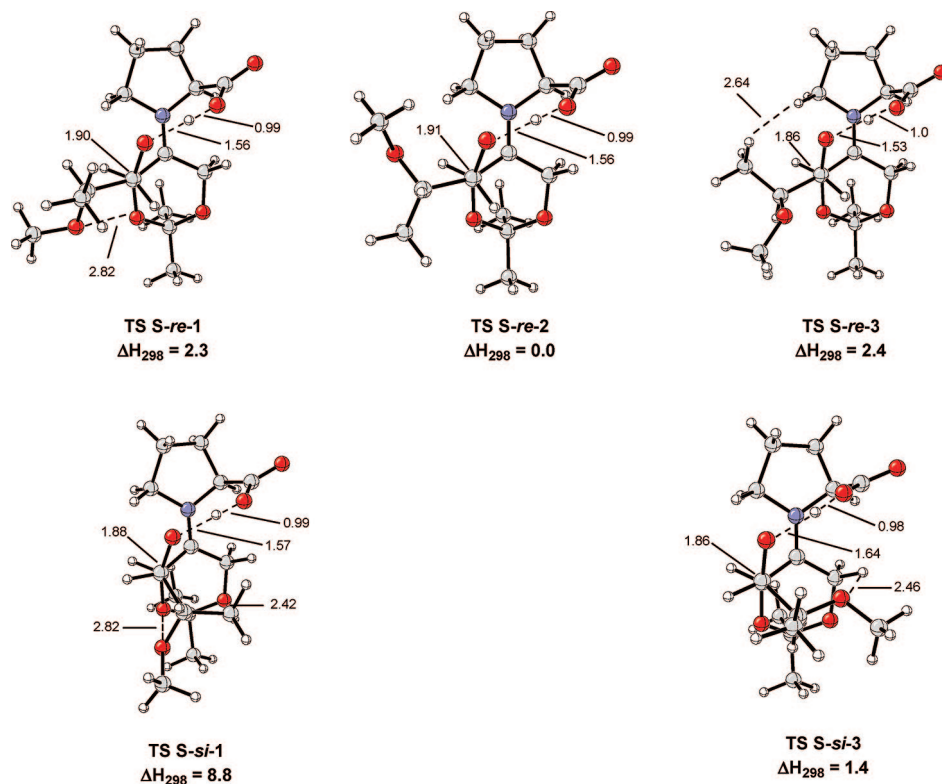
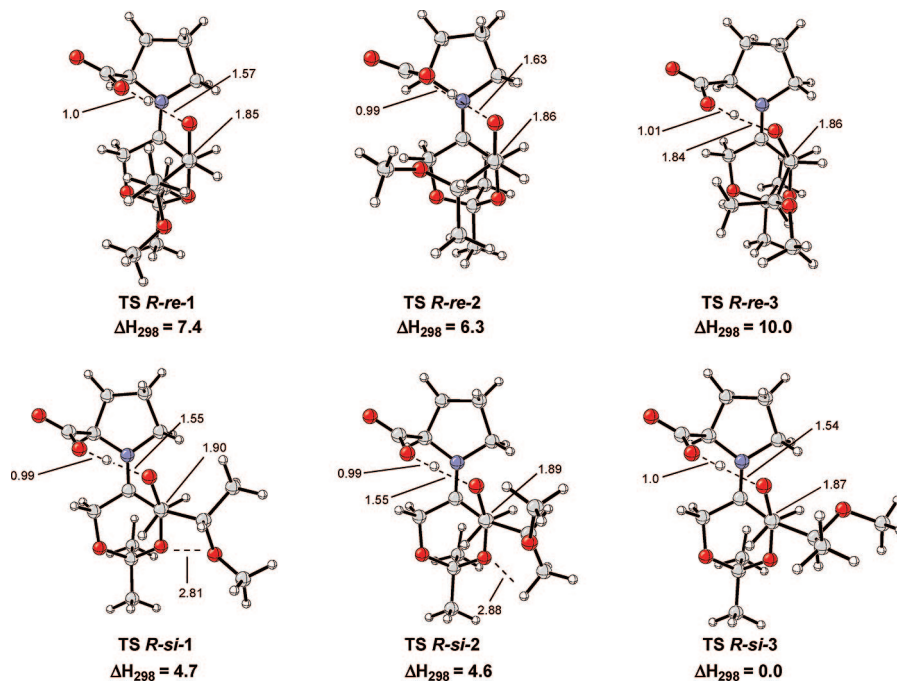


FIGURE 1. Transition state models for the proline-catalyzed aldol reaction.



**FIGURE 2.** Most stable transition structures for aldol reaction of **17** with **19** ( $\Delta H_{298}$  = kcal/mol) from (*S*)-proline. First row structures correspond to *re*-facial attack and the second the *si*-attack. An optimized structure for **TS S-si-2** was not found.



**FIGURE 3.** Most stable transition states for aldol reaction of **17** with **20** ( $\Delta H_{298}$  = kcal/mol) from (*R*)-proline. First row structures correspond to *re*-facial attack and the second the *si*-attack.

the neutral enamine and simultaneous proton transfer from the carboxylic acid to the carbonyl acceptor.<sup>4,11</sup> Transition states with an approximate dihedral angle  $+60^\circ$  (*S*-Pro) and  $-60^\circ$  (*R*-Pro) relative to the carbonyl group and the enamine double bond are favored by almost 10 kcal/mol. Transition states with the carboxylic acid group and the enamine double bond *syn* are 2–10 kcal/mol higher in energy than the transition states

involving the *anti*-enamine (Figure 1a). Only the *anti*-enamine was considered in this study.

It is well-known that the nucleophilic attack follows a partial-Zimmerman-Traxler-like<sup>12</sup> transition state but the metal that forms the sixth atom in the chair is missing. The *re*-face of the acceptor aldehyde, where the aldehyde substituent is located in a pseudoequatorial arrangement, is preferred for the nucleophilic

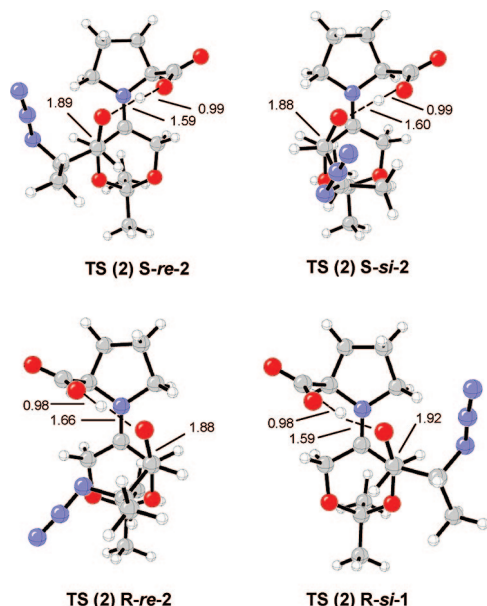


**FIGURE 4.** Most stable transition structures for aldol reaction of **18** with **19** and **20**. First row: (*S*)-proline: *re* (a) and *si* (b) facial attack. Second row: (*R*)-proline: *re* (c) and *si* (d) facial attack.

**TABLE 1.** Predicted and Experimental  $\Delta H$  Values (kcal/mol) for the Transition States of Proline-Catalyzed Reactions (**17** versus **2**, and **18** versus **8**)

	$\Delta H_{298}$ <i>anti/syn</i> predicted for <b>17</b>	$\Delta H_{\text{exp}}$ <i>anti/syn</i> <sup>a</sup> experimental for <b>2</b>	$\Delta H_{298}$ <i>anti/syn</i> predicted for <b>18</b>	$\Delta H_{\text{exp}}$ <i>anti/syn</i> <sup>a</sup> experimental for <b>8</b>
( <i>S</i> )-Proline	1.42	0.95	>3	>3
( <i>R</i> )-Proline	>3	>3	1.15	0.95

<sup>a</sup> Calculated from the ratio of aldol products as determined by <sup>1</sup>H NMR.

attack in the (*S*)-proline transition state. The same reasoning can be applied to the transition states of (*R*)-proline but, in this case, the attack on the *si*-face of the aldehyde places the substituent in equatorial orientation.

First, we examined the TS corresponding to the nucleophilic attack of **19** and **20** on (*S*)-aldehyde **17**.

As shown in Figure 2, the most stable transition state [TS *S-re-2*] involves the addition of the *anti*-enamine to the *re*-face of **17**. The *si*-face attacks are disfavored due to the steric interactions between the substituents of **17** and the enamine of **19**. Other *re*-face attack TS [TS *S-re-1*] and [TS *S-re-3*] are higher in energy than [TS *S-re-2*] because the former involves repulsion between the oxygens of the methoxy group of the aldehyde and the enamine, and the latter involves the repulsion between the largest group (Me) and the proline-ring.

The transition states with (*R*)-proline are shown in Figure 3. In the transition structures involving the (*R*)-proline enamine, the facial selectivity of **17** switches as compared to the (*S*)-proline case, and now the *si*-face attacks are favored. A *re*-face attack involves substantial steric interactions between the enamine and the substituents of **17**. The most stable transition structure is [TS *R-si-3*]. This transition structure is more stable than analogous [TS *R-si-1*] and [TS *R-si-2*] due to the steric interactions between the oxygen of **20** and either the oxygen or methyl of **17**.

The stereoselectivity is lower in the case of (*S*)-proline (Figure 2), as compared to (*R*)-proline (Figure 3), because there is steric

repulsion between the methyl of **17** and the enamine of **19** in [TS *S-re-2*] that is not present in [TS *R-si-3*].

This hypothesis was confirmed from a similar theoretical study with model  $\alpha$ -azide-aldehyde, **18**. The most stable transition structure in this case was also one in which there was minimal steric interaction between the proline enamine and the aldehyde substrate (Figure 4).

In Table 1, the computational results involving the model systems shown in Scheme 3 are compared with experimental results. There is an excellent agreement between the computed and the experimental stereoselectivity.

In conclusion, as previously reported, the stereoselectivity of the aldol reaction catalyzed by proline is governed by the preference for a transition state where the aldehyde substituent is located in a pseudoequatorial position (partial-Zimmerman-Traxler transition state). However, when an aldehyde bearing a  $\alpha$ -stereogenic center is used as acceptor, steric factors have been shown to be determining from the computational evidence obtained. The reaction catalyzed by (*R*)-proline follows the normal Felkin-Anh course, with nucleophilic attack *anti* to the largest group, the medium group inside, and the smallest outside, as in TS *R-si-3*; however, with (*S*)-proline, this TS is sterically hindered, and a lower (mismatched) stereoselectivity is observed. HF/6-31G(d) has shown to be an excellent method/basis set for these calculations.

## Experimental section

**General Procedure for the Catalytic Asymmetric Aldol Reaction of Ketone **3** and Aldehyde **8** Using (*R*)- or (*S*)-Proline.** A solution of (*R*)- or (*S*)-proline (5.5 mg, 0.048 mmol) in DMF (0.2 mL) was stirred for 24 h. Afterward, ketone **3** (0.13 g, 1 mmol) was added, and the mixture was allowed to react for 3 h. Then, aldehyde **8** was added portionwise (0.10 g, 0.48 mmol) in three additions of 0.16 mmol solved in 33  $\mu$ L of DMF during 48 h. After the last addition, the mixture was stirred at room temperature for 96 h. Then, NH<sub>4</sub>Cl (sat) (1 mL) was added and the mixture was extracted with AcOEt (3  $\times$  2 mL). The organic layer was dried (Na<sub>2</sub>SO<sub>4</sub>) and the solvent was evaporated. The residue was purified by column chromatography (hexane/AcOEt 4:1). Yields and *anti/sin* diastereoselectivities are shown in scheme 3.

**(3*S*,4*S*,5*R*)-5-Azido-6-*O*-benzyl-1,3,4-trihydroxy-1,3-*O*-isopropylidene-hexan-2-one (**14**).** Column chromatography (hexane/AcOEt 4:1). [ $\alpha$ ]<sub>D</sub><sup>25</sup> -22.1° (*c* 0.14, CH<sub>2</sub>Cl<sub>2</sub>); <sup>1</sup>H NMR (300 MHz, CDCl<sub>3</sub>, 298 K):  $\delta$  7.4–7.3 (m, 5H), 4.7–4.5 (m, 2H), 4.38 (dd, *J* = 8.7, 1.5 Hz, 1H), 4.28 (d, *J* = 17.7 Hz, 1H), 4.07 (d, *J* = 17.7 Hz, 1H), 4.0–3.9 (m, 1H), 3.9–3.8 (m, 2H), 3.76 (d, 1H, *J* = 3.9 Hz), 1.51 (s, 3H), 1.41 (s, 3H). <sup>13</sup>C NMR (75 MHz, CDCl<sub>3</sub>, 298 K):  $\delta$  212.5 (C), 138.1 (C), 128.9 (CH), 128.3 (CH), 127.4 (CH), 101.9 (C), 74.1 (CH<sub>2</sub>), 72.5 (CH), 70.3–70.2 (CH, CH<sub>2</sub>), 66.9 (CH<sub>2</sub>), 60.8 (CH), 23.9 (CH<sub>3</sub>), 23.8 (CH<sub>3</sub>). EM (IES-EM): *m/z* 358.0 [*M*<sup>+</sup> + 23]; Anal. Calcd. for C<sub>16</sub>H<sub>21</sub>N<sub>3</sub>O<sub>5</sub>: C, 57.30; H, 6.31; N 12.53. Found: C 57.28; H 6.21; N 12.86.

**(3*R*,4*R*,5*R*)-5-Azido-6-*O*-benzyl-1,3,4-trihydroxy-1,3-*O*-isopropylidene-hexan-2-one (**16**).** Column chromatography (hexane/AcOEt 4:1). [ $\alpha$ ]<sub>D</sub><sup>25</sup> +25.1° (*c* 0.7, MeOH); <sup>1</sup>H NMR (300 MHz, CDCl<sub>3</sub>, 298 K):  $\delta$  (major isomer) 7.4–7.3 (m, 5H), 4.7–4.5 (m, 2H), 4.39 (dt, *J* = 8.7, 1.5 Hz, 1H), 4.28 (d, *J* = 17.7 Hz, 1H), 4.09 (d, *J* = 17.7 Hz, 1H), 4.0–3.9 (m, 1H), 3.9–3.8 (m, 2H), 3.77 (dd, *J* = 3.9, 1.5 Hz, 1H), 1.51 (s, 3H), 1.41 (s, 3H). <sup>13</sup>C NMR (75 MHz, CDCl<sub>3</sub>, 298 K):  $\delta$  (major isomer) 212.5 (C), 137.8 (C), 128.8 (CH), 128.1 (CH), 127.2 (CH), 101.8 (C), 73.8 (CH<sub>2</sub>), 72.3 (CH), 70.1–70.0 (CH, CH<sub>2</sub>), 66.7 (CH<sub>2</sub>), 60.7 (CH), 23.8 (CH<sub>3</sub>), 23.7 (CH<sub>3</sub>). EM (IES-EM): *m/z* 358.0 [*M*<sup>+</sup> + 23]; Anal. Calcd. For C<sub>16</sub>H<sub>21</sub>N<sub>3</sub>O<sub>5</sub>: C, 57.30; H, 6.31; N 12.53. Found: C 57.25; H 6.27; N 12.72.

**(2R,3S,4R,5S)-3,4-dihydroxy-2,5-bis(hydroxymethyl)pyrrolidine hydrochloride [2,5-dideoxy-2,5-imino-D-galactitol (15) •HCl].** To a solution of **14** (0.055 mmol) in MeOH (2.5 mL), Pd/C (10%) was added (20 mg). The suspension was stirred under H<sub>2</sub> (45 psi) during 18 h at room temperature. Afterward, conc. HCl (0.3 mL) was added, and the mixture was stirred under H<sub>2</sub> (45 psi) for 6 h at room temperature. After this time, the reaction mixture was filtered through Celite, and the solvent was evaporated to give **15**. Spectroscopic data for **15** are consistent with those described in the literature. <sup>13</sup>C EM (IES-EM): *m/z* 164.1 [M<sup>+</sup>-Cl<sup>-</sup>], 217.3 [M<sup>+</sup> +

23]; Anal. Calcd. for C<sub>6</sub>H<sub>14</sub>ClNO<sub>4</sub>: C, 36.10; H, 7.07; N, 7.02. Found: C, 36.38; H, 7.02; N, 7.35.

**Acknowledgment.** We thank Dr. F. R. Clemente, Dr. C. D. Anderson, and C. Y. Legault for their helpful discussions and suggestions and the UCLA Academic Technology Service and CESGA for computer resources. F.C. and E.G.D. thank Ministerio de Educación y Ciencia and CSIC for predoctoral fellowships (BQU2001-1503 and I3P-BPD2005, respectively). Financial support by the Spanish Government is gratefully acknowledged (grant CTQ2004-03523/BQU).

(10) All the transition states were fully optimized and characterized by frequency analysis at the HF level of theory with the 6-31G(d) basis set as implemented in Gaussian 98 (see Supporting Information for a complete author list). Previous work in related reactions has shown the efficiency of this method and this basis set: Ha-Yeon Cheong, P.; Ahang, H.; Thayumanavan, R.; Tanaka, F.; Houk, K. N.; Barbas, C. F. *Org. Lett.* **2006**, *8*, 811–814. Enthalpies,  $\Delta H_{298}$ , were computed for the gas phase.

(11) (a) Clemente, F. R.; Houk, K. N. *Angew. Chem., Int. Ed.* **2004**, *43*, 5766–5768. (b) Bahmanyar, S.; Houk, K. N.; Martin, H. J.; List, B. *J. Am. Chem. Soc.* **2003**, *125*, 2475–2479. (c) Bahmanyar, S.; Houk, K. N. *J. Am. Chem. Soc.* **2001**, *123*, 11273–11283. (d) Bahmanyar, S.; Houk, K. N. *J. Am. Chem. Soc.* **2001**, *123*, 12911–12912.

(12) Zimmerman, H. E.; Traxler, M. D. *J. Am. Chem. Soc.* **1957**, *79*, 1920–1923.

**Supporting Information Available:** Experimental details for the synthesis of compounds **8**. <sup>1</sup>H and <sup>13</sup>C NMR copies of new compounds. Cartesian coordinates of all reported structures. This material is available free of charge via the Internet at <http://pubs.acs.org>.

JO800934B

(13) (a) Singh, S.; Han, H. *Tetrahedron Lett.* **2005**, *45*, 6349. (b) Doyagüez, E. G.; Calderón, F.; Sánchez, F.; Fernández-Mayoralas, A. *J. Org. Chem.* **2007**, *72*, 9353–9356.